# Quantum oscillations in the photocurrent of GaAs/AlAs *p-i-n* diodes

E. E. Vdovin,[1,2] M. Ashdown,[1] A. Patanè,[1] L. Eaves,[1] R. P. Campion,[1] Yu. N. Khanin,[2] M. Henini,[1] and O. Makarovsky[1,*]

[1]*School of Physics and Astronomy, University of Nottingham, Nottingham NG7 2RD, United Kingdom*

[2]*Institute of Microelectronics Technology RAS, 142432 Chernogolovka, Russia*

(Received 25 November 2013; revised manuscript received 10 April 2014; published 12 May 2014)

We report large amplitude quantum oscillations and negative differential conductance in the bias voltage-dependent photocurrent of *p-i-n* GaAs diodes with an AlAs barrier in the intrinsic (*i*) region. The oscillations appear only when the devices are illuminated with above-band gap radiation. They are strongly suppressed by a weak (∼2 T) in-plane magnetic field. Their period, amplitude, and magnetic field dependence are explained in terms of the quantized motion of confined photoexcited electrons and holes in the triangular potential wells formed by the AlAs barrier and the strong electric field in the intrinsic region. With increasing electric field, the energy levels of the electrons (holes) successively reach the top of their confining potentials, thus leading to a larger overlap of their wave functions with the free carriers in the *p*- (and *n*-) doped electrodes and to the observed oscillatory modulation of the recombination rate and photocurrent as a function of the applied voltage. The effect on the photocurrent oscillations amplitude of placing a layer of InAs quantum dots in the AlAs barrier layer is also examined.

DOI: 10.1103/PhysRevB.89.205305 PACS number(s): 73.50.Pz, 73.63.Hs, 73.40.Kp, 72.20.Ht

## I. INTRODUCTION

Semiconducting *p-i-n* junctions are widely used as nuclear particle detectors [1] and have many applications in optoelectronics. Photoexcited carriers created in the intrinsic (*i*) region of the device are rapidly swept out by the strong built-in electric field. This field is further increased by applying a large reverse bias, which can lead to impact ionization of carriers, an effect exploited in avalanche photodetectors [2,3]. The science and technology of this type of device has been further advanced by band-structure engineering methods. By incorporating various combinations and compositions of potential barriers, quantum wells, and/or quantum dot layers into the intrinsic region of the device, it has proved possible to fine tune the carrier dynamics, capture and recombination processes, and to exploit tunneling and confinement effects for applications in photonic and quantum information processing. For example, *p-i-n* diodes have been used as single photon emitters [4], and as sensitive photodetectors in which a single photoexcited carrier localized in a quantum well or at a quantum dot can produce a significant change in the conductance of the device [5–11].

Under certain conditions the photoresponse of semiconducting materials and devices can reveal a variety of different quantum-oscillatory phenomena. A classic example, namely the energy relaxation of photoexcited electrons and holes by the emission of approximately monoenergetic optical phonons, leads to multiple oscillations of the photocurrent as a function of the photon energy of the light excitation source [12]. There are also many reports of oscillations in the electrical conduction of devices as a function of the applied bias voltage due to optical phonon emission [13], or to the quantization of the energy of the carrier motion by confining potential barriers. For example, resonant tunneling into the quasibound states of wide quantum wells can give rise to a large number of well-defined peaks in the differential conductance [14]. Similar quantum confinement effects have also been observed in optically excited multiquantum well heterostructures with *p-n* junctions [15]. Here we report oscillations in the photocurrent of GaAs *p-i-n* diodes containing a single AlAs barrier in the undoped, intrinsic layers. These oscillations have features which are qualitatively different from previous observations and originate from quantized ballistic motion of photoexcited electrons and holes.

Our investigation of photocurrent oscillations are made on a series of GaAs *p-i-n* diodes in which an AlAs potential barrier is located in the intrinsic (*i*) GaAs layer; two of the heterostructures were grown with a layer of self-assembled InAs quantum dots (QDs) placed in the middle of the AlAs barrier. Bias-dependent photocurrent (PC) measurements were carried out over a wide range of bias, temperature, and in high magnetic fields applied either parallel or perpendicular to the direction of current flow. They reveal the presence of more than 20 resonant peaks with regions of negative differential conductance in the PC over temperatures ranging from 4 to 80 K with a modulation amplitude of up to 20% of the total current. We identify two distinct series of oscillations. In Sec. V of the paper we explain how these two series arise from the quantized motion of ballistic photoexcited electrons and holes in their respective triangular potential wells that are formed by the AlAs barrier potential and the strong electric field in the central intrinsic GaAs layer. The energy levels of the bound subbands in each quantum well are sensitive to the magnitude of the electric field, which can be increased to values of up to $2 \times 10^7$ V m$^{-1}$ when a large reverse bias is applied. This field is two orders of magnitude larger than that for which intervalley transfer of hot electrons is observed in GaAs transferred electron devices [16]. Such a large field can accelerate electrons to an energy of ∼1 eV above the Γ-conduction band minimum when they hit the AlAs barrier layer of our device.

We describe how confined electron (and hole) energy levels with high quantum numbers successively reach the top of the triangular potential as the electric field is increased. This causes the tails of their Airy-type wave functions near the classical turning point of the potential to overlap strongly with the high

*Corresponding author: oleg.makarovsky@nottingham.ac.uk

 

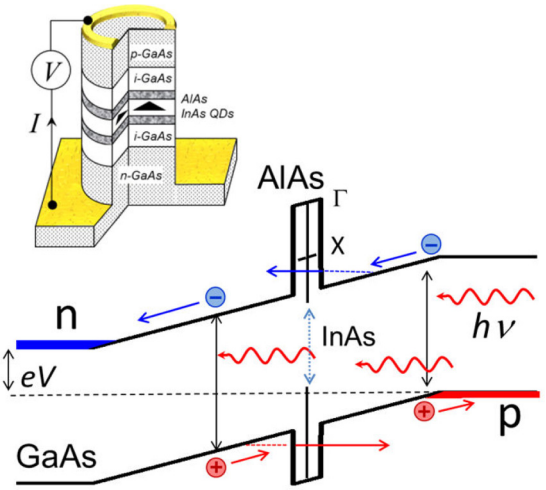


FIG. 1. (Color online) Schematic band diagram of a *p-i-n* device with a tunnel barrier in the intrinsic ($i$) region at a forward applied bias $V = +0.5$ V; it shows the motion of photoexcited carriers. A schematic diagram of the mesa structure is shown in the inset.

density of free majority carriers in the nearby $p$- (and $n$-) doped electrodes. The resulting enhancement of the recombination rate leads to a modulation of the measured photocurrent as a function of applied bias voltage. We confirm the quantum nature of the photocurrent oscillations by studying the effect of an applied magnetic field and by developing a model which provides a good fit to the measured oscillatory periods. By studying a range of devices we find that the amplitude of the photocurrent oscillations is enhanced in devices which contain a layer of InAs QDs in the barrier layer and we suggest a possible mechanism for this behavior. Our results demonstrate that a significant fraction of the photoexcited carriers travel ballistically in the strong electric field, with kinetic energies of up to 1 eV and mean free paths in excess of 100 nm, without emitting optical phonons or undergoing intervalley transitions into the higher conduction band minima of GaAs.

## II. DEVICE CHARACTERISTICS

Our devices are GaAs *p-i-n* diodes with a 10-nm-thick AlAs barrier located close to the middle of the intrinsic ($i$) region. The heterostructures were grown by molecular beam epitaxy on heavily doped (001) $n$-type substrates at a growth temperature of 550 °C. A schematic band diagram and details of the layer composition of our devices are presented in Fig. 1 and Table I. In two of the devices (devices A and B), a layer of self-assembled InAs QDs (sheet density $\sim 10^{11}$ cm$^{-2}$) was grown at the center of the AlAs barrier; a control sample with no QD layer (device C) was also grown, thus allowing us to study how the QD layer affects the photocurrent oscillations. Details of the layer composition of the devices are given in Table I. The heterostructure layers were processed using standard optical lithography into circular mesa devices with a diameter of 200 $\mu$m, see inset of Fig. 1. A ring-shaped metallic contact on the top $p$-doped electrode provides a circular window through which light from a laser can be used to photoexcite carriers across the band gap of the GaAs layers.

## III. EXPERIMENTAL RESULTS

When the device is illuminated with photons with an energy that exceeds the band gap of GaAs, photoexcited electrons and holes are generated in the undoped GaAs layers on each side of the AlAs tunnel barrier. The charged carriers drift in opposite directions in the presence of the electric field $F_z$, as shown in Fig. 1. A photocurrent is generated when one of the pair of photoexcited carriers can surmount or tunnel through the barrier and the other carrier drifts to the opposite electrode. We adjust the strength of $F_z$ by applying a bias voltage $V$ to the junction; $F_z$ is zero (the so-called flat band condition) when the forward bias is set at $V = V_{\rm FB} \approx 1.5$ V. At a reverse bias of $V = -3$ V, $F_z \sim 2 \times 10^7$ V m$^{-1}$. The current-voltage characteristics $I(V)$ are strongly asymmetric with respect to forward and reverse bias, as expected for a *p-i-n* device. At bias voltages below $\sim +1$ V through to reverse biases of $-3$ V, the dark current remains low ($<10$ pA for a 200-$\mu$m-diameter mesa at reverse bias, $V = -2$ V).

Figure 2 shows the effect of different levels of optical illumination on the current-voltage characteristics of device A (containing a QD layer in the AlAs barrier) with above band gap radiation over a wide range of bias voltage. Superimposed upon the monotonic variation of photocurrent with bias is a series of oscillatory peaks with an amplitude which is a significant fraction (up to $\sim$20%) of the total photocurrent. No oscillatory structure is observed in the absence of illumination. We observe the oscillations over a wide range of wavelengths from close to the GaAs band gap value of $\lambda = 850$ nm to $\lambda = 650$ nm. At low powers, a single series of oscillations, labeled "electrons," appears with a typical peak-to-peak voltage interval $\Delta V$ of between $\sim$100 and 300 mV, depending on the intensity of illumination, and extending over the bias range $-3 < V < 1$ V, see Fig. 2. In addition, at high illumination intensities, a second series of oscillations, labeled "holes" is observed, with significantly smaller period, ranging from $\sim$20 to 100 mV, and extending over a narrower bias voltage range from around zero bias up to $\sim$1 V. We explain the significance

TABLE I. Layer composition of the diodes.

| | Device A | Device B | Device C |
|---|---|---|---|
| $p^+$-GaAs | | 500 nm at $2 \times 10^{18}$ cm$^{-3}$ GaAs | |
| Undoped GaAs | 60 nm | 30 nm | 60 nm |
| Undoped AlAs | 10 nm, InAs QD layer in central plane of the barrier | | 10 nm |
| Undoped GaAs | | 100 nm | |
| $n$-GaAs | | 100 nm of $2 \times 10^{16}$ cm$^{-3}$ | |
| $n^+$-GaAs | | 1 $\mu$m of $4 \times 10^{18}$ cm$^{-3}$ | |

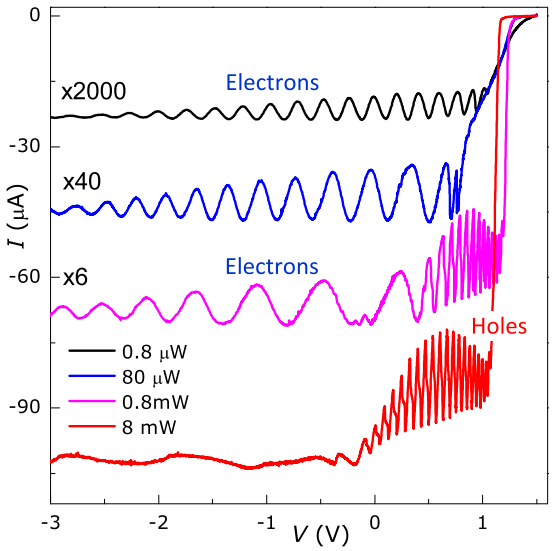


FIG. 2. (Color online) $I(V)$ characteristics for device A, showing the oscillatory photocurrent at low temperature (4 K) for different levels of laser illumination ($\lambda = 633$ nm).

of these labels in Sec. IV of the paper. Figure 3 shows the bias dependence of the period $\Delta V$ on bias voltage and illumination intensity for both series of oscillations observed in device A. Note that the $\Delta V$ for both the electron and hole series is largest at high reverse bias and that it increases slightly with the level of illumination.

To gain a qualitative insight into the physical origin of the oscillations, we investigated the effects on the oscillations of temperature and applied magnetic field. Their amplitudes decrease when the temperature of the device is increased and the oscillations disappear entirely at ~80 K, see Fig. 4(a); the oscillatory period is effectively independent of temperature. This suggests that the oscillations arise from a quantum effect

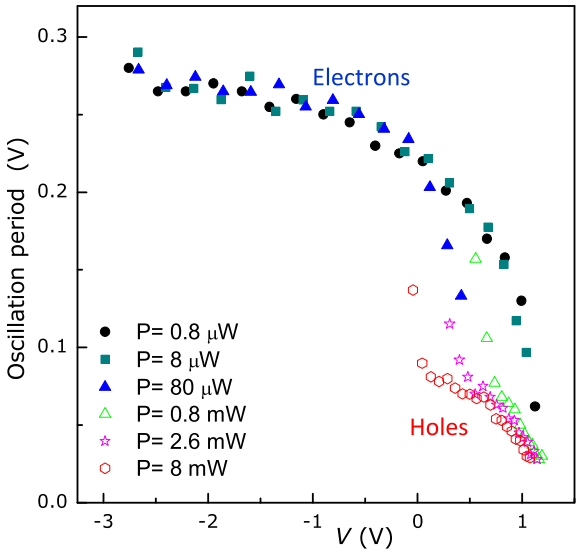


FIG. 3. (Color online) Dependence of the peak-to-peak oscillation period $\Delta V$ as a function of bias voltage $V$ and of laser intensity $P$ for device A.

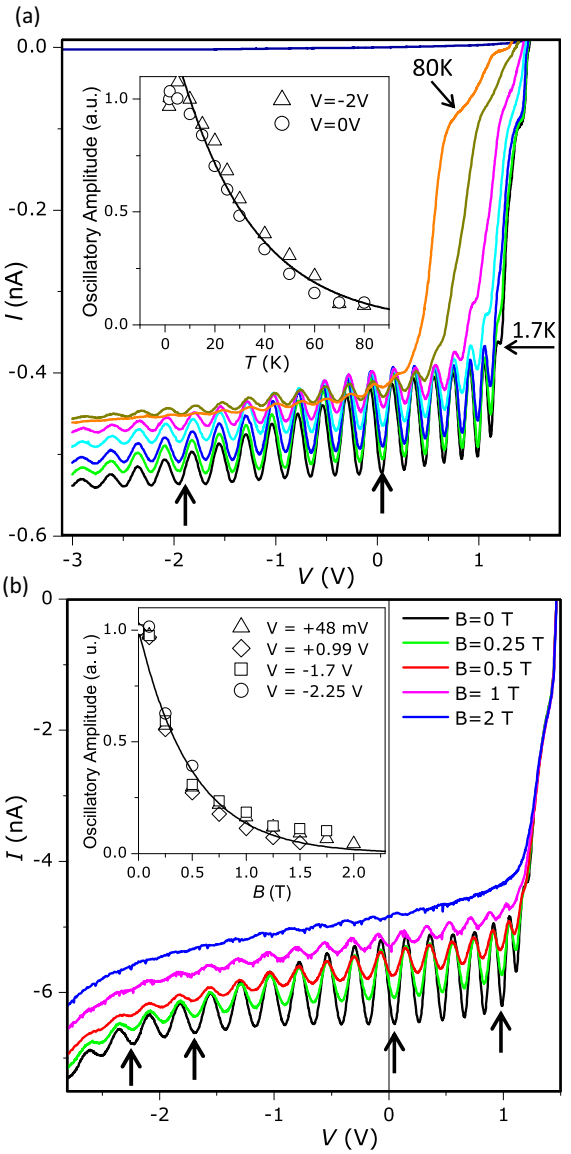


FIG. 4. (Color online) (a) Temperature dependence of the oscillatory photocurrent of device A (bottom to top curves 1.7, 5, 10, 20, 50, 70, and 80 K). The inset shows the decrease of the oscillation amplitude as a function of temperature. (b) Dependence of the oscillatory photocurrent of device A on magnetic field $B = B_x$, applied perpendicular to the current flow (i.e., parallel to the plane of the tunnel barrier). The inset shows the decrease of the oscillation amplitude as a function of $B_x$ for various bias voltages. The vertical arrows indicate the bias voltages selected for the plots of oscillatory amplitude shown in the insets.

which is quenched by level broadening, phonon scattering, or thermal activation when the temperature is increased.

As shown in Fig. 4(b), for device A, the oscillatory amplitude also decreases markedly when a magnetic field is applied perpendicular to the direction of current flow (parallel to the plane of the barrier) and the oscillations disappear at fields in excess of 2 T. In contrast, when the magnetic field is applied parallel to the direction of the current flow, the oscillation amplitude is maintained, even at fields of 12 T. The Lorentz force exerted by a perpendicular magnetic field

on the high velocity ballistic carriers has a strong effect on their classical trajectories and the corresponding quantum states. The quenching of the amplitude of the oscillations in a weak perpendicular magnetic field therefore suggests that they are associated with the ballistic, i.e., scattering-free, motion of charged carriers across the triangular potential well, over distances of several tens of nanometers. Long electron mean free paths have been reported in previous studies of GaAs/(AlGa)As double barrier resonant tunneling devices (RTDs) for which high energy electrons were observed to traverse undoped quantum wells of widths up to 120 nm without scattering [14,17]. We also note that we observed no photocurrent oscillations in similar *p-i-n* devices made from six other wafers in which the thickness of the intrinsic layers on each side of the barrier exceeds ~100 nm, suggesting that the carrier dynamics cease to be ballistic over such length scales.

To investigate the possibility that the photocurrent oscillations are related directly to the layer of quantum dots in the AlAs barriers in device A, we also investigated the properties of two other heterostructures: One (device B) also contains a QD layer in the AlAs barrier, but has a thinner intrinsic layer on the $p$ side of the AlAs barrier, and the other (device C) contains no InAs QDs. Otherwise, all the devices have a similar layer composition (Table I). As shown in Fig. 5, all three devices exhibit photocurrent oscillations under illumination, though the oscillations are most pronounced in devices A and B containing a QD layer. The significance of the quantum number index $j_m$ used in Fig. 5 will be discussed in the next section. By comparing the "electron" photocurrent oscillations of devices A and B at the same photoexcitation power (8 $\mu$W) in Figs. 5(a) and 5(b), it can be seen that the oscillatory period is larger in device B. The physical origin of this difference is due to the difference in the width of the undoped GaAs layer on the right-hand side of the AlAs barrier (see Fig. 1), as explained in the next section of the paper.

We also carried out capacitance-voltage measurements at low temperatures (4 K) over the bias range $-3 < V < 1$ V, where the dc current is small; these data allowed us to determine the bias dependence of the thickness of the depletion layers in the doped $n$ and $p$ layers adjacent to the intrinsic region, thus providing us with a good estimate of the bias dependence of the electric field in the undoped GaAs layers (see Supplementary Material for details [18]). These results were used in the model described in the next section.

## IV. ANALYSIS

To understand the physical origin of the photocurrent oscillations, we now consider the quantum mechanics of carriers moving in the triangular potential well formed by the quantum well potential barrier and the strong electric field in the undoped GaAs layers. This is illustrated in Fig. 6(a), which shows the quantization of the electron motion along the direction of current flow. A similar diagram applies for the hole states confined in the triangular valence band potential on the other side of the AlAs barrier, but with a smaller energy spacing due to the larger hole mass. At low levels of photoexcitation ($\lesssim 1$ $\mu$W), the space charge density induced by the photoexcited carriers is relatively small and, for a particular bias voltage, we assume a constant electric field $F_z$ in the intrinsic regions on each side of the barrier layer. We can then model carrier quantization in the formed potential wells by using analytical solutions of the Schrödinger equation for an infinite triangular quantum well (TQW). The quantization energies $E_j$ and eigenfunctions $\psi_j(z)$ due to the $z$ component

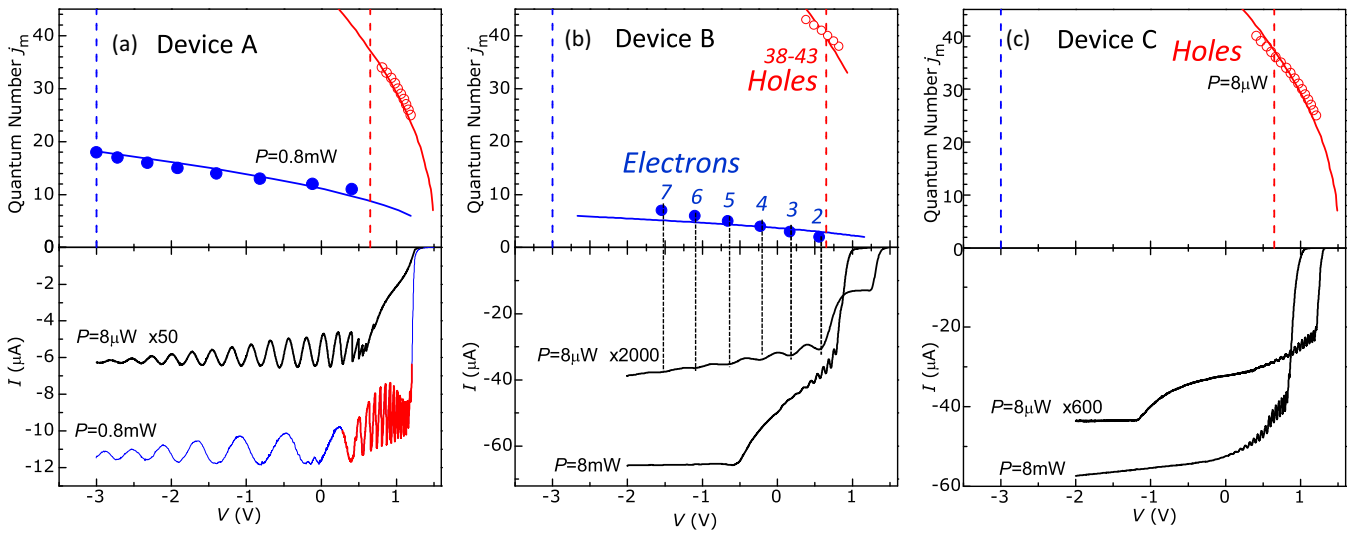


FIG. 5. (Color online) Lower row of plots: Photocurrent oscillations at $T = 6$ K for devices A, B, and C. Upper row of plots: Bias voltage positions and quantum numbers $j_m$ assigned to the photocurrent peaks associated with photoexcited electrons (blue symbols) and holes (red symbols) confined in the triangular quantum wells on $p$ and $n$ sides of the AlAs barrier. In (a) the values of electron and hole $j_m$ values for device A are obtained by fitting the "blue" and "red" parts of the oscillating $I$-$V$ curve, taken at a photoexcitation power $P = 0.8$ mW. Here $j_m$ is the quantum number of the highest energy bound state of the triangular potential well at a particular bias voltage. In (b) blue and red numbers indicate calculated values of $j_m$ for the electrons and holes corresponding to the observed photocurrent resonances. The dashed blue (red) line indicates the bias voltage at which the conduction (valence) band edge in the doped $n$ (and $p$) regions becomes aligned with the top of the conduction (and valence) band AlAs barrier (see also Fig. 6).

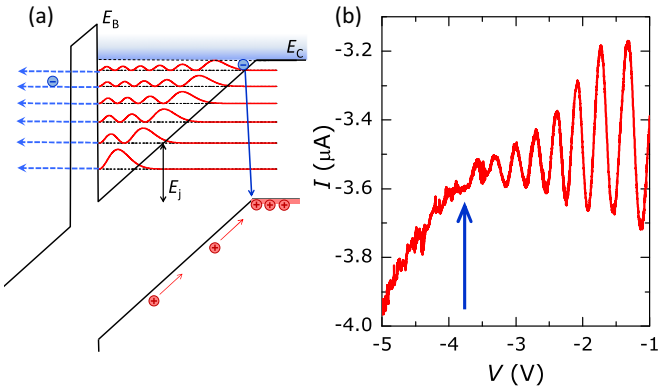


FIG. 6. (Color online) (a) Schematic diagram illustrating the Airy function eigenstates and the mechanism proposed to explain the photocurrent oscillations. Photoexcited electrons occupy the quantized energy subbands $j$ of the triangular potential well (a similar diagram applies to the hole states on the other side of the barrier). With increasing electric field, the energy of the uppermost subband $j_m$ approaches the top of the potential well $E_C$, and eventually ionizes, joining the continuum states above the well; the increasingly strong overlap of the probability density of the electron eigenstate with the high density of free holes in the $p$-doped electrode leads to an increase in the rate of electron recombination with the holes (shown schematically by the downward solid arrow) and hence to a decrease in the photocurrent due to tunneling through the AlAs barrier. (b) A plot of the photocurrent oscillations at large reverse bias for device A at $P \sim 100$ $\mu$W. The blue arrow indicates the last observable photocurrent maximum, corresponding to the energy alignment of $E_C$ and $E_B$ in (a).

of the carrier motions are

$$E_j \sim \left(\frac{\hbar^2}{2m^*}\right)^{1/3}\left[\frac{3\pi e F_z}{2}\left(j+\frac{3}{4}\right)\right]^{2/3} \quad (1)$$

and

$$\psi_j(z) = \mathrm{Ai}\left[\frac{2m^* e F_z}{\hbar^2}\left(z - \frac{E_j}{eF_z}\right)\right]. \quad (2)$$

Here $j = 0,1,2,\ldots$ is the subband quantum number, and the eigenfunctions $\psi_j(z)$ are given by Airy (Ai) functions [19]. Each state $j$ gives rise to a two-dimensional subband of states in which the carriers move freely in the $xy$ plane parallel to the barrier layer. We can treat the quantum states in a TQW as long-lived quasistationary eigenstates since the carrier "dwell time" is much longer than the time required to make a transit of the TQW. This is because the transmission coefficient of the 10 nm AlAs barrier (see Table I for the layer structure) is low so, in semiclassical terms, the carriers "bounce" off the barrier many times before they are transmitted through it by tunneling. Indeed, our observation of the well-resolved oscillatory structure requires that the quantized states are long-lived standing waves rather than dynamic, energy broadened wave packets.

We use the known values of the electron ($m_e^* = 0.067m_e$) and heavy hole ($m_h^* = 0.35m_e$) effective masses in GaAs to determine the energies of the quantum states as a function of $F_z$. Using this approximation, we can determine the electric field values and hence the applied bias voltage $V$ at which a particular excited state subband with quantum number $j_m$ and energy $E_{j_m}$ reaches the top of the triangular quantum well at which point it becomes "ionized" and joins the continuum of extended electronic states above (and below) the conduction (and valence) band edge in the doped electrodes. The voltage interval $V_j - V_{j+1}$, over which successive $(j+1)$th and $j$th levels reach the ionization energy, can then be estimated and compared with the measured voltage interval $\Delta V$ between the peaks of the photocurrent plotted in Fig. 2. The sequence of $j_m$ values is determined by the best fit to the data. This analysis provides a good fit to the $\Delta V$ values of both the longer-period oscillatory structure (labeled "electrons") and the higher-frequency oscillations ("holes") – see the three upper boxes in Fig. 5, which compares the measured data points with the calculated values of $V_j - V_{j+1}$ for the electron and hole states in all three samples.

As can be seen by comparing the lower boxes in Figs. 5(a) and 5(b), for the same laser excitation power (8 $\mu$W) the electron oscillations in device B have longer period $\Delta V$ than in device A due to the smaller width of the TQW (30 nm) for device B. This leads to stronger quantum confinement and to a larger energy separation of the quantized electron subbands.

We attribute the increase in the measured period of the oscillations at high illumination intensities (Fig. 3) to an electrostatic effect. With increasing intensity of illumination, the electrical space charge of photoexcited carriers, which accumulate close to the barrier at the bases of the two triangular potentials, becomes significant. The photoexcited holes have a lower barrier transmission coefficient than electrons due to their heavier effective mass and tend to accumulate either on the left side of the barrier or in the quantum dots within the barrier. At high photoexcitation levels the positive space charge of these holes results in an increase in the electric field in the triangular potential well for the photoexcited electrons on the $p$-type side and in a corresponding reduction of the field on the $n$-type side of the barrier at a particular fixed bias. Therefore, to maintain a given set of values for the subband energies $E_j$, with increasing levels of photoexcitation, it is necessary to compensate the electrostatic effect of the photoexcited holes by an increment of applied bias voltage $V$, thus leading to the observed increase of $\Delta V$ (see Supplementary Material for details of this mechanism [18]).

We propose the following physical mechanism to explain the observed oscillatory modulation of the photocurrent. As $F_z$ is increased, a particular electron Airy function state $j$ approaches the top of its triangular potential well and its wave function increasingly overlaps with the high density of majority holes in the doped $p$-GaAs electrode, see Fig. 6. This overlap increases the recombination rate of the photoexcited electrons in the $j_m$th subband, thus reducing their contribution to the photocurrent by their tunneling through the AlAs barrier. As the voltage is varied, successive Airy function energy levels approach the top of the potential well and join a continuum of extended, unbound states in the GaAs conduction band. Hence the competition between tunneling and the bias-dependent modulation of the recombination rate repeats itself, giving rise to the observed oscillatory photocurrent.

The corresponding mechanism for the photoinduced holes confined in their Airy function states on the other side of the

barrier can explain the hole series of oscillations with shorter period $\Delta V$, which occurs over the bias voltage range from $\sim$0 to 1 V for high illumination intensities. The smaller $\Delta V$ (see Figs. 2, 3, and 5) of the hole oscillations is due to the larger effective mass of the photoexcited heavy holes and the smaller level spacing between the Airy function eigenenergies, see Eq. (1). We observe no clear evidence of oscillations due to light holes.

A notable feature of the photocurrent measurements is that the electron and heavy hole-related oscillations appear over extended, but different, ranges of bias voltage. Our electrostatic model can account for this behavior by taking into account the values of the conduction and valence band discontinuities at the GaAs/AlAs interfaces of the tunnel barrier. For the electrons, the $\Gamma$-conduction band discontinuity at the AlAs/GaAs interface is large, $\sim$1 eV, whereas holes are restrained by a smaller valence band discontinuity of 0.6 eV [20]. At small forward bias, $V < 0.5$ V, the energies of hole states with large $j$ quantum numbers start to exceed the top of the AlAs valence band barrier. In addition, the overlap between the tails of their wave functions with the majority electrons in the $n$-doped layers is small, since the classical turning point of the hole wave function is several nanometers away from the edge of the $n$-GaAs layer. Under these conditions, the holes in these states tunnel rapidly through the barrier and their recombination rate with majority electrons in the $n$-GaAs layer is too low to modulate the photocurrent.

In contrast, as shown in Fig. 6(b), the photocurrent oscillations due to electrons disappear at reverse bias voltages in excess of $-3.5$ V. At this large reverse bias the energy of the conduction band edge at the $p$-GaAs electrode coincides with that of the $\Gamma$-conduction band edge $E_b$ of the AlAs barrier layer, i.e., $E_b = E_c$ in Fig. 6(a). At higher values of reverse bias the highest energy states in the triangular potential well are no longer confined by the AlAs barrier so the photocurrent increases rapidly with increasing reverse bias, see Fig. 6(b).

The persistence of the oscillations up to $-3.5$V indicates that the AlAs barrier has a high reflection coefficient for incident electrons even for energies well above that of the $X$-conduction band minimum of AlAs ($E_X \sim 0.3$ eV [20]). At sufficiently large forward bias, around 1.1 V, somewhat below the "flat-band" condition, the electron oscillations disappear. The likely explanation for this behavior is that the electric field in the intrinsic region becomes too weak to produce well-resolved Airy functionlike quantized states for the electrons, due in part to their slower transit time across the triangular well at these low $F_z$ values.

## V. DISCUSSION

Our model allows us to quantify the dynamics of the carrier motion in the strong electric field in the intrinsic region. In Fig. 6(a) the well-defined "standing wave" quantum states with high quantum numbers correspond, in a semiclassical "particle" description, to carriers moving ballistically back and forth across the well, with mean free paths of $\sim$100 nm. The time $\tau$ for a single ballistic transit of the well is given semiclassically by the relation $\tau \sim \hbar k_z^*/eF_z$, where $\hbar k_z^*$ is the (crystal) momentum of the carrier when it hits the barrier. Using the band dispersion curves $\varepsilon(k_z)$ of GaAs [21] and the relation $\varepsilon(k_z^*)_{e,h} = \Delta E_{e,h}$, we can estimate $\tau_{e,h}$ for the bias value at which a carrier hits the AlAs barrier with an energy close to the barrier height $\Delta E_{e,h}$. This gives $\tau_e \sim 6 \times 10^{-14}$ s at $V = -3$ V and $\tau_h \sim 3 \times 10^{-13}$ s at $V = +0.6$ V. In both cases, the associated periods $2\tau_{e,h}$ of the quantized carrier motion in the subbands are less than the characteristic time $\tau_{\mathrm{LO}}$ for the emission of a longitudinal optic (LO) phonon by hot carriers, namely 0.3 ps for electrons and $\sim$3 ps for holes [22]. Indeed, in our model the condition $2\tau_{e,h} < \tau_{\mathrm{LO}}$ is a requirement for observation of the quantum oscillations.

It is also interesting to note that when a reverse bias $V = -3$ V is applied, the electric field in the intrinsic region is $F \sim 2 \times 10^7$ V m$^{-1}$ and the conduction electrons hit the AlAs barrier with a kinetic energy of $\sim$1 eV. These values of $F$ and of the kinetic energy $\varepsilon_{\max}$ greatly exceed those of GaAs Gunn diodes ($F = 3 \times 10^5$ V m$^{-1}$ and $\varepsilon_{\max} \sim 0.3$ eV [16]). Despite the large electric fields in our devices, we see no evidence of electrons undergoing intervalley transfer, so it appears that a significant fraction of the electrons can attain energies of up to 1 eV in the $\Gamma$-conduction band valley, without undergoing scattering into the higher band minima.

It is necessary to consider the possibility that the oscillatory structure arises from the sequential emission of optic phonons by hot electrons or holes, of the type observed in the current-voltage characteristics of single barrier (AlGa)As-GaAs diodes [13,23,24]. Those oscillations have a constant voltage period given by $\hbar\omega_L/e = 36$ mV, where $\hbar\omega_L$ is the energy of the longitudinal optic (LO) phonon in GaAs. However, they can be observed in "dark," unilluminated conditions and so are unlikely to be the origin of the oscillations in photocurrent which we investigate here. In addition, sequential emission of LO phonons would give an oscillatory period and bias voltage dependence significantly different from what we observe. The quantum confinement effect which we use to explain the photocurrent oscillations are more analogous to the Fabry-Perot-like multiple resonant peaks observed in the dark current-voltage characteristics of RTDs with wide quantum wells [14,17]. In both cases, the oscillations are strongly affected by the application of an in-plane magnetic field.

Finally, we consider how the photocurrent oscillations are influenced by the presence of an InAs QD layer in the AlAs barrier. All three of our devices, whose layer compositions are given in Table I, display the oscillations at low temperatures (see Fig. 5). For devices A and B, which contain a layer of QDs in the barrier, both the electron and hole series of oscillations are observed over a wide range of bias. The period of electron oscillations is larger for device B with a shorter spacer layer on the $p$ side [see Fig. 5(b) and Table I]. Only hole oscillations were observed in device C, which has no QD layer. We note that recent experiments have demonstrated that scattering of carriers at the heterointerface between the (InAl)As QD and the surrounding AlAs matrix strongly affects the radiative recombination of photoexcited carriers [25,26]. A possible explanation for the stronger oscillatory effect in devices A and B is that the QD layer in the barrier gives rise to a scattering potential which enhances elastic scattering-assisted tunneling. The characteristic length scale of this potential is determined partly by the mean in-plane separation, $\sim$10 nm, of the

QDs. Such a potential would allow elastic scattering-assisted tunneling with a change of in-plane wave vector of up to $\Delta k_{\parallel} \sim 10^9$ m$^{-1}$. The model that we have developed to account for the photocurrent oscillations requires that the tunneling and recombination rates of carriers confined in the triangular potential wells compete with each other; hence we postulate that the presence of the QD layer serves to enhance the tunneling rate so that the two rates become approximately matched when a quantized state approaches the top of the potential well.

## VI. SUMMARY AND CONCLUSIONS

We have observed strong quantum oscillations in the low temperature photocurrent-bias voltage characteristics of GaAs *p-i-n* diodes containing an AlAs barrier in the intrinsic region. Their physical origin is shown to be qualitatively different from that due to the sequential emission of optical phonons [13,23,24] or from interwell hopping in *p-i-n* diodes containing multiple quantum wells [15]. We attribute the photocurrent oscillations to the bias-dependent quantization of the ballistic carrier motion in the triangular potential wells by the AlAs tunnel barrier and strong electric field in the intrinsic region of the device. The quantum coherence of these high energy states, which extend over length scales of up to ~100 nm, is not destroyed by LO phonon emission processes, nor by $\Gamma - X$ intervalley transfer. Our results provide insights into the carrier dynamics of photoexcited carriers in *p-i-n* diodes and may therefore be relevant for future applications of this type of device.

## ACKNOWLEDGMENT

We acknowledge the joint support of the Royal Society and Russian Federation for Basic Science (International Exchanges Cost Share Project RS-RFBR 13-02-92612).

[1] R. Ferrini, G. Guizzetti, M. Patrini, F. Nava, P. Vanni, and C. Lanzieri, Eur. Phys. J. B **16**, 213 (2000).
[2] S. Y. Lin, Y. R. Tsai, and S. Ch. Lee, Appl. Phys. Lett. **78**, 2784 (2001).
[3] K. A. Patel, J. F. Dynes, A. W. Sharpe, Z. L. Yuan, R. V. Penty, and A. J. Shields, Electron. Lett. **48**, 111 (2012).
[4] C. L. Salter, R. M. Stevenson, I. Farrer, C. A. Nicoll, D. A. Ritchie, and A. J. Shields, Nature (London) **465**, 7298 (2010).
[5] J. C. Blakesley, P. See, A. J. Shields, B. E. Kardynał, P. Atkinson, I. Farrer, and D. A. Ritchie, Phys. Rev. Lett. **94**, 067401 (2005).
[6] H. W. Li, B. E. Kardynał, P. See, A. J. Shields, P. Simmonds, H. E. Beere, and D. A. Ritchie, Appl. Phys. Lett. **91**, 073516 (2007).
[7] L. Xu, E. Wu, X. Gu, Yi. Jian, G. Wu, and H. Zeng, Appl. Phys. Lett. **94**, 161106 (2009).
[8] B. E. Kardynal, Z. L. Yuan, and A. J. Shields, Nat. Photon. **2**, 425 (2008).
[9] O. Thomas, Z. L. Yuan, and A. J. Shields, Nat. Commun. **3**, 644 (2012).
[10] E. E. Vdovin, O. Makarovsky, A. Patanè, L. Eaves, and Yu. N. Khanin, Phys. Rev. B **79**, 193311 (2009).
[11] O. Makarovsky, E. E. Vdovin, A. Patanè, L. Eaves, M. N. Makhonin, A. I. Tartakovskii, and M. Hopkinson, Phys. Rev. Lett. **108**, 117402 (2012).
[12] R. E. Nahory, Phys. Rev. **178**, 1293 (1969).
[13] T. W. Hickmott, P. M. Solomon, F. F. Fang, F. Stern, R. Fischer, and H. Morkoc, Phys. Rev. Lett. **52**, 2053 (1984).
[14] T. M. Fromhold, L. Eaves, F. W. Sheard, M. L. Leadbeater, T. J. Foster, and P. C. Main, Phys. Rev. Lett. **72**, 2608 (1994).
[15] H. M. Khalil, S. Mazzucato, S. Ardali, O. Celik, S. Mutlu, B. Royall, E. Tiras, N. Balkan, J. Puustinen, V.-M. Korpijärvi, and M. Guina, Mat. Sci. Eng. B **177**, 729 (2012).
[16] S. M. Sze, *Physics of Semiconductor Devices*, 2nd ed. (John Wiley and Sons, New York, 1981).
[17] M. L. Leadbeater, E. S. Alves, L. Eaves, M. Henini, O. H. Hughes, A. Celeste, J. C. Portal, G. Hill, and M. A. Pate, J. Phys.: Condens. Matter **1**, 4865 (1989).
[18] See Supplemental Material at http://link.aps.org/supplemental/10.1103/PhysRevB.89.205305 for capacitance $C(V)$ measurements and charge accumulation at high intensities of light.
[19] M. Abramowitz and I. A. Stegun (eds.), *Handbook of Mathematical Functions*, National Bureau of Standards Applied Mathematics Series No. 55 (US GPO, Washington, DC, 1964).
[20] C. N. Yeh, L. E. McNeil, L. J. Blue, and T. Daniels-Race, J. Appl. Phys. **77**, 4541 (1995).
[21] J. R. Chelikowsky and M. L. Cohen, Phys. Rev. B **14**, 556 (1976).
[22] R. Scholz, J. Appl. Phys. **77**, 3219 (1995).
[23] L. Eaves, P. S. S. Guimarães, B. R. Snell, D. C. Taylor, and K. E. Singer, Phys. Rev. Lett. **55**, 262 (1985).
[24] M. Alikacem, D. K. Maude, L. Eaves, M. Henini, G. Hill, and M. A. Pate, Appl. Phys. Lett. **59**, 3124 (1991).
[25] T. S. Shamirzaev, A. V. Nenashev, A. K. Gutakovskii, A. K. Kalagin, K. S. Zhuravlev, M. Larsson, and P. O. Holtz, Phys. Rev. B **78**, 085323 (2008).
[26] T. S. Shamirzaev, J. Debus, D. S. Abramkin, D. Dunker, D. R. Yakovlev, D. V. Dmitriev, A. K. Gutakovskii, L. S. Braginsky, K. S. Zhuravlev, and M. Bayer, Phys. Rev. B **84**, 155318 (2011).